

MYOGENIC STAGE, SARCOMERE LENGTH AND PROTEASE ACTIVITY MODULATE LOCALIZATION OF MUSCLE-SPECIFIC CALPAIN*

Koichi Ojima,^{1,2} Yasuko Ono,¹ Naoko Doi,^{1,2} Katsuhide Yoshioka,³ Yukiko Kawabata,^{2,3}
Siegfried Labeit,⁴ and Hiroyuki Sorimachi^{1,2}

From ¹Department of Enzymatic Regulation for Cell Function, The Tokyo Metropolitan
Institute of Medical Science, Tokyo 113-8613, Japan

²CREST, JST, Kawaguchi 332-0012, Japan

³Graduate School of Agricultural and Life Sciences, The University of Tokyo, Tokyo 113-8657,
Japan

⁴Institut für Anästhesiologie und Operative Intensivmedizin, Universitätsklinikum Mannheim,
Mannheim 68167, Germany

Running title: Protease activity-dependent myofibrillar localization of muscle-specific calpain

Address correspondence to: Hiroyuki Sorimachi, Department of Enzymatic Regulation for
Cell Function, The Tokyo Metropolitan Institute of Medical Science, Tokyo 113-8613, Japan,
Tel: +81-3-3823-2181; Fax: +81-3-3823-2359; E-mail: sorimach@rinshoken.or.jp

p94/calpain3 is a Ca²⁺-binding intracellular protease predominantly expressed in skeletal muscles. p94 binds to the N2A and M-line regions of connectin/titin, and localizes in the Z-bands. Genetic evidence showing that compromised p94 proteolytic activity leads to muscular dystrophy (LGMD-type) indicates the importance of p94 function in myofibrils. Here, we show that a series of p94 splice variants are expressed immediately after muscle differentiation and differentially change localization during myofibrillogenesis. We found that endogenous N-terminal (but not C-terminal) domain of p94 were not only localized in the Z-bands but also directly bound to sarcomeric α -actinin. These data suggest the incorporation of proteolytic N-terminal fragments of p94 into the Z-bands. In myofibrils, localization of exogenously expressed p94 shifted from the M-line to N2A

as the sarcomere lengthens beyond ca. 2.6 and 2.8 μ m for wild-type and protease-inactive p94, respectively. These data demonstrate for the first time that p94 proteolytic activity is involved in responses to muscle conditions, which may explain why p94 inactivation causes LGMD.

p94/calpain 3 is a member of the calpain family of intracellular Ca²⁺ requiring Cys proteases, which cleave substrates at specific and limited sites to modulate their structure and function. In contrast to the conventional μ - and m-calpains, which are ubiquitously expressed in almost all cells (1,2), p94 is predominantly expressed in skeletal muscle with lesser amounts of several differentially spliced variants in skeletal muscle and nonmuscle cells (3). The human p94 gene, *CAPN3*, was identified as responsible for limb-girdle muscular dystrophy type 2A

(LGMD2A, or “calpainopathy”) (4). In mice, transgenic overexpression of a protease-inactive form of p94, p94:C129S, and p94 gene knock-out caused a mild myopathy and muscular dystrophy, respectively (5-7). Furthermore, a defect in the proper proteolytic activity of p94 is a common feature of LGMD2A pathogenic mutations (8). These findings indicate that p94 protease activity is essential to maintain healthy condition of skeletal muscle. However, the specific physiological functions of p94 as a protease in skeletal muscle remain largely unknown.

Skeletal muscles contain highly organized sarcomere structures, which consist of systematically expressed myofibrillar proteins. One of the earliest myofibrillar proteins expressed in vertebrate myogenic cells is connectin/titin (9), which is the largest protein molecule known, and is abundantly expressed in striated muscles where it constitutes an intrasarcomeric filament (10,11). During sarcomere assembly, connectin is considered a key molecule for integration of thin filament/Z-band precursors (I-Z-I bodies) and the thick filaments, which are independently assembled in growth tips of elongating myotubes. The N-terminus of connectin is located in both I-Z-I body and mature Z, and the C-terminus is in the M-line of the thick filament (12-14). A single molecule of connectin spans a half of the sarcomere from Z to M to integrate the Z-band and the thick filaments, maintaining the location of thick filaments between the Z-bands.

Connectin also plays an important role as a scaffold for its specific ligands such as sarcomeric- α -actinin/ α -actinin 2 (s- α -actinin)

(15,16), T-cap/telethonin (17), muscle-specific RING-finger protein-1 (MURF-1) (18), as well as p94 (19). These proteins interact with connectin at three significant regions in the sarcomeres, namely, Z-bands, N2A and M-line regions, where highly organized protein complexes form. p94 directly interacts with connectin at both N2A and M (19). Interaction between p94 and connectin at N2A stabilizes p94, which otherwise autolyzes very rapidly, thus, connectin may regulate p94 proteolytic functions (20,21). p94 has been also detected in Z (19,22), although a molecular basis for anchoring p94 in Z is unknown. Thus, p94 exists in all three regions in sarcomeres, suggesting that p94 may contribute to myofibril organization in cooperation with other connectin ligands and/or connectin.

This study aims (1) to characterize the spatiotemporal expression and localization of p94 and its splicing variants during skeletal muscle differentiation in relation to connectin, (2) to identify p94 interacting molecules in the Z-band components, and (3) to clarify the role of the proteolytic activity of p94 in the unique context of muscle cells. Detailed immunohistochemical study using primary cultures of skeletal muscle cells revealed that p94 and its splice variants differ in their expression and localization during maturation of sarcomere structures. It was also demonstrated that correlation between localization of p94 and sarcomere lengths exists, which, at least in part, involves its protease activity.

Experimental procedures

Experimental animals - All procedures used

for experimental animals were approved by the Experimental Animal Care and Use Committee in the Tokyo Metropolitan Institute of Medical Science. C57BL/6 mice were purchased from Nihon CLEA Inc.

Preparation of mouse skeletal muscle cell -

Mouse skeletal muscle cells were prepared as previously described (23). Isolated myogenic cells were cultured on Matrigel (BD Bioscience) coated Labtech chamber slides (Nalge Nunc International Inc.) or 60 mm dishes (Asahi Techno Glass) in growth medium (20% FBS, and 0.2 μ M ascorbic acid (Wako Pure Chemical Industries Ltd.), in Dulbecco's modified Eagle's medium (DMEM)). To induce muscle differentiation, the medium was switched to differentiation medium (5% horse serum (Invitrogen), and 0.2 μ M ascorbic acid in DMEM) for further culture. All media were supplemented with 100 U/ml penicillin, 0.1 mg/ml streptomycin, and 2 mM L-glutamine (Invitrogen).

RT-PCR analysis - Total RNA was prepared from cultured muscle cells from the quadriceps femoris and the soleus muscles of 15-week-old C57BL6 mice, using TRISOL (Invitrogen) according to the manufacturer's instructions. First strand cDNA was synthesized from 5 μ g of total RNA using a First Strand Synthesis kit (GE Healthcare Bio-Sciences Corp.). Primers used to detect p94, splicing variants of p94, connectin, and μ -calpain are shown in Table I. The cycle number for PCR was 25 for all samples.

Western blot analysis - Cells were harvested in the presence of the homogenizing buffer (20 mM Tris/Cl (pH 8.0), 0.1 mM EDTA (pH 8.0), 1 mM DTT, 28 μ M E64, 20 μ g/ml

soybean trypsin inhibitor and 2 mM PMSF). The amount of protein was quantified with a DC RC protein assay kit (Bio-Rad Laboratories Inc.). Equal amounts of protein from each sample were subjected to SDS-PAGE. Gels were transferred onto Immobilon-P transfer membrane (Millipore Corp.). After blocking, membranes were incubated with antibodies against p94 (anti-pIS2C antibody, 1:1000; further purified anti-pIS2 antibody (21) using the C-terminal part of the pKrich peptide (24), i.e., NH₂-VKKKKKNKPIIFVC-COOH), embryonic MHC (clone F1.652, 1:50; Developmental Studies Hybridoma Bank (DSHB), University of Iowa), or desmin (1:1000; Sigma). An affinity-purified rabbit anti-p94:ex15⁻16⁻ antibody was generated using the KLH-conjugated peptide SVDRPVPRPGHT-C, corresponding to the sequence encoded by transcript of exons 14 and 17 of the mouse p94 gene. Subsequently, membranes were incubated with peroxidase-conjugated secondary antibodies (1:10; Nichirei Inc.), followed by visualization of reacted bands using a POD immunostaining kit (Wako Pure Chemical Industries Ltd).

Immunofluorescent staining - Cultured cells and muscle tissues were fixed and then stained as previously described (23). For muscle tissues, longitudinal cryostat sections (7 μ m) of EDL muscles from six-month-old C57BL/6 mice were made. Antibodies used in immunofluorescence studies were affinity-purified goat anti-pIS2C antibody (1:300), mouse anti-s- α -actinin antibody (1:1000; Sigma), affinity-purified chicken

anti-connectin N2A antibody (1:500; (25)), affinity-purified rabbit anti-connectin M8M9 antibody (1:300; (26)), rabbit anti-p94 NS antibody (1:300; (24)), and affinity-purified rabbit anti-p Δ ex15/16 antibody (1:300; this study). Alexa-488- or Alexa-555-conjugated secondary antibodies were used (Molecular Probes Inc., Eugene, OR). Nuclei were stained with TOTO3 or DAPI (4, 6-diamidino-2-phenylindole dihydrochloride) (Molecular Probes). Specimens were analyzed on a laser scanning confocal microscopic system (LSM 510; Carl Zeiss Inc.), which employed a Zeiss Axiovert inverted microscope with a Plan-Apochromat 63 \times (NA 1.4) lens. Images were recorded and processed with LSM510 imaging software.

Yeast two-hybrid screening - The cDNA sequence corresponding to the NS domain of human p94 (nt: 307–531 of NM_000070, aa: 1–75) was cloned into pGBKT7 (Clontech). The bait plasmid and a human skeletal muscle cDNA library (HL4010AB, Clontech) were cotransformed into *Saccharomyces cerevisiae* AH109, according to the manufacturer's instructions. About 9×10^6 transformants were screened on selection medium plates, SD-LWHA, at 30°C, yielding 20 grown colonies. Prey plasmids were isolated from these colonies and subjected to DNA sequencing. Three prey plasmids were confirmed for their reproducibility, two of which encoded s- α -actinin (corresponding to aa 441–568 in ACTN2), and the other one encoded von Willebrand factor (vWF). As vWF is an extracellular protein secreted by endothelial cells (27), we did not further analyze if vWF indeed interacts with p94 *in*

vivo. Thus, only s- α -actinin was further analyzed as to its interaction with p94.

cDNA constructs for expression in mammalian cells - The cDNA corresponding to full-length human p94, mouse p94 variants lacking exon 6 and/or exons 15 and 16 (p94 Δ exX), and their protease-inactive forms, p94:C129S (p94CS) and p94 Δ exX:CS, were cloned into pcDNA3.1/N-FLAG vector (28). The NS domain of human p94 was cloned into pEGFP-C1 (Clontech). The cDNA for human s- α -actinin 2 (nt: 174–2921 of NM_001103, aa: 1–894) with an N-terminal Myc-tag was cloned into pcDNA3.1 (Invitrogen).

Immunoprecipitation - Expression vectors for Myc-tagged human s- α -actinin and Flag-tagged human p94 or GFP-tagged human p94 NS were transfected into COS7 cells. Cells were harvested 72 hr after electroporation and then homogenized in lysis buffer (0.5% digitonin, 50 mM CsCl, 10 mM Triethanolamine, 1 mM EDTA, 2 mM phenylmethylsulfonyl fluoride, 10 μ g/ml aprotinin, pH 7.8). Cell lysates were centrifuged at 20,000 $\times g$ for 15 min, and the supernatants preincubated with protein G sepharose (GE Healthcare Bio-Sciences) to absorb nonspecific binding proteins. After centrifugation, the supernatants were incubated with anti-Myc antibody (9E10; DSHB), ANTI-FLAG M2 affinity gel (Sigma), or anti-GFP antibody (JL-6, Clontech). After incubation with protein G sepharose for 60 min, which was omitted when ANTI-FLAG affinity gel was used, immunocomplexes were collected by centrifugation. The resin was washed with an

excess amount of lysis buffer followed by elution of immunoprecipitated proteins with SDS sample buffer.

Transfection into primary skeletal muscle cells - Transfection was performed using TransIT-LT1 transfection reagent (Mirus Inc.). On the indicated day, cells were fixed and analyzed by immunofluorescent staining. Quantitative comparison of different sarcomeric localization was performed by the following formula: M-line (N2A) accumulation (%) = the number of sarcomeres which presented accumulation of Flag-tagged p94 in M-lines (N2A region)/total number of counted sarcomeres. Sarcomere length was measured as the distance between the centers of adjacent M-lines, which is positive for connectin M8M9, using Zeiss LSM imaging software. Calculated ratios were resorted according to sarcomere lengths. In cultured cells expressing p94WT, p94CS, p94 Δ ex6:WT, and p94 Δ ex6:CS, 108, 107, 47, and 86 sarcomeres, respectively, were counted.

RESULTS

Transcription of the p94 gene during myofibrillogenesis

Expression of p94/calpain 3 and its splicing variants during myofibril development was analyzed by detecting corresponding transcripts in primary mouse skeletal muscle cell culture. As previous studies have revealed that mouse embryonic muscles express p94 variants without exons 6, 15, and/or 16 (29), the relative abundance of transcripts resulting from those exon-skipping events was

examined (Fig. 1 A). Differentiation of cultured cells was confirmed by decreased expression of embryonic myosin heavy chain (MHC) compared with the expression of desmin (Fig. 1 B), and by the formation of sarcomere structures (see below). In proliferating presumptive myoblasts (PM), i.e., cells before the onset of differentiation, p94 and its splicing variants were hardly detected (Fig. 1, C–F, PM). Predominating among the tested p94 splice isoforms, transcripts for full-length p94 (Fig. 1 A, FL) became detectable immediately after induction of muscle differentiation, and was observed throughout muscle maturation (Fig. 1, C–F, arrows). Splice isoforms lacking exon 6 (Fig. 1A, Δ ex6) were recognized from day 1 to 13 (Fig. 1D, open arrowhead). Splice isoforms lacking exons 15 and 16 (Fig. 1 A, Δ ex15/16) were also observed from day 1 to 13, but the amount relative to the transcripts with exons 15 and 16 (Fig. 1 A, ex15/16⁺) was very low (Fig. 1 E, open arrowhead). The expression of variant transcripts without exons 6, 15, and 16 (Fig. 1 A, Δ ex6/15/16) was slightly detected at day 3 (Fig. 1 F). All tested adult skeletal muscles only expressed a full-length p94, i.e., no exon-skipping variants were detectable (Fig. 1, C–F, QC and Sol). In contrast, transcripts of the μ -calpain large subunit gene showed constant expression in all samples (Fig. 1 G), consistent with its proposed nature as a housekeeping gene (30).

Changes in the protein amounts of p94 isoforms during myofibrillogenesis

Next, the expression of protein products

corresponding to the p94 transcripts detected above was examined. No 94 kDa full-length p94 protein was detected in cells cultured under proliferating conditions (Fig. 1 H, PM). Immediately after the induction of differentiation, full-length p94 was detected (Fig. 1 H, arrow), and the amounts of protein were not downregulated during myofibrillogenesis. In addition, the amounts of protein in the faster migrating bands—possible proteolytic fragments of p94—decreased, suggesting that the stabilization of p94 is facilitated as myofibrillogenesis proceeds (Fig. 1 H, closed arrowheads). In adult skeletal muscles, the predominating full-length p94 is coexpressed with lower amounts of shorter isoforms or proteolytic fragments (Fig. 1 H, QC).

Based on molecular size, the 89 kDa band (Fig. 1 H, open arrowhead) could be variants lacking either exon 6, 15 and/or 6, or proteolytic fragments of full-length p94. Therefore, an anti-p Δ ex15/16 antibody specific for p94 isoforms lacking exons 15 and 16 (Δ ex15/16) were raised by using a peptide spanning the exons 14 to 17 junction of the mouse p94 as an antigen (Fig. 1, A and D). The antibody detected the 89 kDa bands (Fig. 1 I), and its protein amount gradually decreased during myofibril maturation. In contrast to the results of RT-PCR, anti-p Δ ex15/16 antibody recognized the 89kDa band in PM, suggesting that p94 Δ ex15/16 protein might not quickly be degraded and accumulate in PM cells even though the corresponding mRNA expression was extremely low (Fig. 1 C, E, and F). Together, our transcriptional and western

studies indicate that p94 Δ ex isoforms are expressed in immature myotubes, whereas full-length p94 constantly accumulated throughout muscle differentiation.

Constant expression of the two p94 binding sites in connectin/titin during muscle differentiation

p94 binds to connectin/titin at I82–I83 in the N2A region and at is7 in the M-line (Fig. 2 A) (31,32). Thus, expression of these regions was also investigated in cultured skeletal muscle cells. N2A connectin was expressed at all stages examined (Fig. 2 B). The 559 bp transcripts corresponding to the M-line region with is7 (is7⁺) were also constantly expressed (Fig. 2 C). The 256 bp bands encoding is7-lacking molecules and (is7⁻) were faintly detected in cultured cells. Consistent with previous reports on muscle fiber type dependent expression of is7 (12); both is7⁺ and is7⁻ variants were expressed at similar levels in the quadriceps femoris, which predominantly consists of fast twitch myofibers, whereas is7⁺ predominated in the soleus, composed of both fast and slow myofibers (Fig. 2 C). These results indicated that the two p94 binding sites in connectin are almost constantly provided during muscle differentiation.

Cytosolic but not sarcomeric localization of p94 during early myofibrillogenesis

To clarify when p94 is incorporated into specific positions within myofibrils, localization of p94 in cultured myotubes at different stages were analyzed. At day 3, s- α -actinin was observed as punctuated

pattern, i.e. the I-Z-I bodies, in emerging growth tips where de novo synthesized myofibrillar proteins are assembled into sarcomere structures (14,33) (Fig. 3 A, brackets), and Z-band striations were seen in the shaft of the same myotubes (Fig. 3 A, arrows). Conversely, using an anti-pIS2C antibody, p94 was detected as small granules in the cytosol of whole myotubes without colocalization with s- α -actinin (Fig. 3, B, E, and H).

The relationship between p94 and connectin localization was explored by staining myotubes using two different anti-connectin antibodies. The anti-N2A antibody (antigen map in Fig. 2 A) detected grainy signals in the growth tips, and striated patterns in the shaft of some myotubes (Fig. 3 D, bracket and arrows). An anti-M-line connectin (M8M9, antigen map in Fig.2A) antibody detected striated signals in the shaft of myotubes, but none in the growth tips (Fig. 3 G, arrows and brackets). No colocalization of p94 with these two regions of connectin was observed (Fig. 3, F and I). At this stage, p94 signals were also detected in myonuclei (Fig. 3, B and H). In summary, p94 was not localized in the Z-bands including the I-Z-I bodies, in the N2A regions, or in the M-lines at this stage, while s- α -actinin and connectin were already organized in striated patterns.

p94 is targeted to the N2A regions and the M-lines in the later stages of myofibrillogenesis

At day 6 of culture, more than 90% of myotubes showed typical myofibrillar protein localization, with s- α -actinin, connectin N2A,

and M8M9, at their proper locations—Z, N2A, and M, respectively. p94 was still detected in the cytosol as granular structures, as seen at day 3, in more than 80% of myotubes, and, infrequently, the localization of p94 precisely coincided with the localization of connectin M8M9.

At day 10, embryonic MHC was hardly detected in cultured cells by western blot analysis (Fig. 1 B), indicating that the cells had become almost fully mature myotubes. In these mature myotubes, in addition to the cytosolic distribution, two main types of p94 positive structures were observed. One was M-line striations coinciding with M8M9 signals (Fig. 3, P-R, arrowheads and arrows). The other was in the I-bands, possibly in the N2A regions (Fig. 3, M-O, brackets and arrows). Intensity in the M-lines was stronger than that in the I-band staining. Localization of p94 in Z was not significant (Fig. 3, J-L). These results indicate that p94 is incorporated into myofibrils after the sarcomere structures are fully mature, through association with above mentioned regions of connectin.

Distinct localization of p94 isoforms in sarcomeres

As shown above, expression of p94 Δ ex15/16 was restricted in developing myotubes (see Fig. 1, E, F, and I). Thus, the localization of p94 Δ ex15/16 was examined in cultured myotubes at day 6 (Fig. 4, A-C). The anti-p Δ ex15/16 antibody captured fuzzy thick striations, which almost overlapped with the s- α -actinin signals at Z (Fig. 4, E and F, brackets), or doublets around Z (Fig. 4, H and I, arrowheads). These data indicate that

p94 Δ ex15/16 is probably localized to N2A or somewhere between Z and N2A. In addition, p94 Δ ex15/16 was found in M (Fig. 4 E, open arrowheads). Contrary to the anti-pIS2C antibody results, the anti-p Δ ex15/16 antibody stained N2A/Z more strongly than M. These results suggest that in developing myotubes, not only the expression but also the localization of p94 isoforms are regulated in a way distinct from that for the full-length p94.

The p94 NS domain is localized in the Z-bands

As shown previously, p94 was detected in Z, especially by antibodies against the p94 N-terminus (19,22). However, clear Z localization of p94 was not detected in cultured skeletal muscle cells with the anti-pIS2C antibody. When the cells at day 6 of culture were stained using the anti-pNS antibody, which was elicited against the N-terminus of p94 (NS region), the Z-band structure was detected in the shaft of relatively mature myotubes (Fig. 5, A–C, arrows and arrowheads), indicating that a p94 fragment containing at least the NS region exists in Z. In contrast, much less, if any, staining at N2A and M was obtained with this antibody. The anti-pNS antibody also detected small granular structures in the cytosol of myotubes (Fig. 5 B), which were not colocalized with s- α -actinin.

The localization of p94 in adult skeletal muscles was also examined with anti-pIS2C and anti-pNS antibodies. Anti-pIS2C antibody labeled preferentially N2A (Fig. 5 E, closed arrowheads), leaving Z less intensely stained (asterisk), whereas both Z and N2A were

stained with the anti-pNS antibody (Fig. 5 H, closed arrowheads and asterisk). In both cases, signal intensity was less in M (Fig. 5, E and H, open arrowheads). In summary, p94 is localized in Z, N2A and M in both maturing muscle cells and skeletal muscle tissues. It is noteworthy, however, that antibodies raised against distinct regions of p94 showed different propensity for staining in those three regions, suggesting that some proteolytic fragments of p94 are associated with the sarcomere structure.

s- α -actinin binds to p94 through the NS region

To identify p94 binding molecules, yeast two-hybrid (YTH) screening was carried out. A middle region of s- α -actinin (corresponding to amino acids (aa) 441–568 in ACTN2) was identified from the human skeletal muscle cDNA library as a binding partner for the p94 NS region. Using a series of truncation mutants of s- α -actinin, it was shown that the original clones identified by the screening encoded the minimal binding site for the p94 NS region, which corresponds to the region spanning the C- and N-terminal halves of the second and third spectrin-like repeats, respectively (Fig. 5 J).

As interaction between the full-length molecules of p94 and s- α -actinin was not detected in YTH, coimmunoprecipitation analysis was carried out. Myc-tagged s- α -actinin and Flag-tagged p94CS, a proteolytically inactive missense (C129S) mutant, were coexpressed in COS7 cells, and subjected to immunoprecipitation with either anti-Myc or anti-Flag antibody. Interaction

between p94 and s- α -actinin was demonstrated in both immunoprecipitations (Fig. 6, A and B). The p94 NS region fused to GFP was also shown to interact with s- α -actinin (Fig. 6, C and D). These results indicate that p94 directly interacts with s- α -actinin via the NS region, which comprises at least a part of the mechanism for its Z localization.

Protease-activity-independent targeting of p94 to specific positions in myofibrils

It was of interest whether the proteolytic activity and/or the molecular structure of p94 affects its targeting to the specific positions in the sarcomeres. Therefore, Flag-tagged p94 and its splicing variants with and without proteolytic activity were expressed in cultured skeletal muscle cells to examine their localization. Six days after transfection, cells expressing Flag-tagged wild-type p94 (p94WT) gave signals one-third to one-tenth less than those observed for cells expressing protease-inactive Flag-p94:C129S (p94CS). This is possibly due to p94WT disappearing by autolysis more rapidly than p94CS, and/or that the excess amount of expressed p94WT is cytotoxic for myotubes. Both p94WT and p94CS were mainly incorporated into the M-lines (Fig. 7, B, E, and H, closed arrowheads). Other p94 variants, such as p94 Δ ex6, p94 Δ ex15/16, p94 Δ ex6/15/16, with and without the CS mutation, showed trends essentially identical to those of p94WT and p94CS (unpublished data). Myotubes expressing excess amount of p94CS and other inactive variants did not show any defect in assembling striated myofibrils. These results

indicate that exogenously expressed p94 and its variants are targeted to the same specific position in the myofibrils as endogenous p94 is, and that proteolytic activity was not required for the process.

Stretch- and protease-activity-dependence of myofibrillar targeting of p94

To compare the behavior of p94WT and p94CS in a more dynamic aspect, the localization of exogenously expressed p94 was evaluated in relation to sarcomere lengths, i.e., the extent of contraction/extension. p94WT and p94CS were preferentially targeted to M in short, contracted sarcomeres (Fig. 7, B and H). In stretched sarcomeres, they were more localized to N2A (Fig. 7 E). p94 variants such as p94 Δ ex6 and p94 Δ ex6:CS (Fig. 7, K and N) showed the same trends. Plotting the frequency of detecting p94 in N2A or M against sarcomere lengths allowed more quantitative assessment; more than 50% of Flag-p94WT was detected in M when sarcomeres were shorter than 2.6 μ m, while in the longer sarcomeres, N2A localization was predominant (Fig. 8 A). Interestingly, we found subtle but significant differences when comparing the stretch-dependent targeting of p94CS with WT. For p94 CS, the threshold length was elongated to 2.8 μ m (Fig. 8 B). Similarly, for p94 Δ ex6, higher stretch levels were required for redistribution from M to N2A for the CS mutant (2.2 vs 2.6 μ m; Fig. 8, C and D). In summary, our results indicate that p94 targets to M in relaxed and/or contracted myofibrils, and is redistributed into N2A by a stretch-dependent mechanism.

Targeting into N2A requires higher amounts of stretch for the proteolytically inactive p94 mutants.

DISCUSSION

In this study, the distinctive features of the expression and localization of p94 and its splicing variants during myofibrillogenesis in the primary culture of skeletal muscle cells, and a novel interaction between the p94 NS region and α -actinin are shown. Furthermore, we have shown that the localization of exogenously expressed p94 changed in correlation with sarcomere length, with p94 proteolytic activity required for this response. This potentially indicates that cellular localization of p94 and possibly of its proteolytic activity is regulated in a stretch-dependent manner.

Fig. 9 A summarizes p94 localization according to developmental stages of myofibrillogenesis. I: in the early stage, I–Z–I and thick filaments are independently assembled; II: by day 6, fundamental myofibrillar components are incorporated into sarcomeres; III: in the late stage), myotubes are fully mature; IV: adult skeletal muscle comprises mature myofibers. Both p94 and its isoforms (p94 Δ ex) are distributed in the cytosol with no myofibrillar localization (Fig. 9A, I). Then, some Z and M localization is observed, although the majority of the protein remains cytosolic (II). Later, p94 isoforms are mainly targeted to N2A, while IS2- and NS-containing fragments respectively accumulate in M/N2A and Z (III). In adult tissues, both NS- and IS2-containing p94 is

found in N2A, but no p94 isoform was detected in the sarcomeres (IV). Previously, the IS2 epitope was detected at both Z and N2A in adult myofibrils (19), which is different from the results shown here, that is, localization mainly at N2A and faintly at M. This is probably because a more specific, affinity-purified anti-pIS2C antibody was used in this study.

Regulation of p94 in the cytosol on its autolysis and targeting to Z/N2A/M

p94 targets to Z/N2A/M after the assembly of basic sarcomere components. By day 3 of differentiation of cultured myotubes, clear striation of Z, N2A, and M, containing α -actinin and connectin, is detected, but p94 is predominantly distributed in the cytosol as small granules. This observation raises at least two questions worthy of further investigation. One is what molecules other than unproteolyzed p94 are contained in these granules, as the signals—detected by both anti-pNS and -pIS2C antibodies—were distinct from the diffuse staining of soluble enzymes. Another is how targeting of p94 to Z, N2A, or M is protected at this developmental stage, even if binding molecules of p94 have already existed and been assembled into sarcomere structures. One reason could be that there is transitional steric hindrance masking binding sites when many different sarcomere components are dynamically incorporated into myofibrils. After day 6 in culture, it is notable that two of the p94 regions, NS and IS2, showed distinct localizations; NS was almost exclusively in Z while IS2 was in N2A and/or M. One

interpretation of these results is that the N- and C-terminal fragments were generated by proteolysis, presumably by autolysis, and targeted to Z and N2A/M, respectively. It is also possible that the affinity to Z or N2A/M of NS or the respective remaining fragments could be much stronger than that of full-length p94. Data showing that NS binds to α -actinin and that the region close to IS2 interacts with N2A connectin (21) are consistent with this idea.

In the same day 6 culture, exogenously expressed Flag-p94WT and -p94CS showed almost identical localization—mainly in N2A/M rather than in Z. This suggests that p94 proteolytic activity is not required for p94 targeting, and that p94 molecules detected at N2A/M possess both NS and IS2 regions—these are undegraded p94 molecules. It may be possible that the affinity of NS to Z is blocked by the extra Flag-tag sequence allowing most of the nonproteolyzed Flag-p94 to be targeted to N2A/M. Still, there should be a mechanism in the cytosol so that exogenously expressed p94 does not exhaustively autolyze.

In more mature myofibrils—at day 10 in culture, and in adult skeletal muscle—NS and/or IS2 epitopes become detectable in Z, N2A, and M. Thus, it is suggested that mature muscle cells facilitate more efficient targeting of nonproteolyzed p94 to those three sites in the sarcomeres.

Altogether, these results suggest the existence of unidentified molecules/mechanisms that regulate the activity of p94 in the cytosol. As p94 Δ ex proteins are expressed in amounts similar to p94 at the early stages of myotube

development, it is tempting to consider that the interaction between p94 and p94 Δ ex is one of the mechanisms that regulates p94, in both its protease activity and targeting. Later, in mature muscle cells, where sarcomere structures gain more integrity and complexity, other mechanisms might allow rapid targeting of p94 to myofibrils and/or suppress its autolysis until being targeted to myofibrils.

Regulated expression of p94 Δ ex during muscle development and its relevance

One of the p94 variants, p94 Δ ex15/16, was shown to be transiently expressed and predominantly incorporated into N2A only in immature myotubes, but not in adult skeletal muscles. Developmental changes of p94 Δ ex/p94 ratios at Z, N2A, M, and in the cytosol are schematically shown in Fig. 9 B. Interestingly, we detected larger amounts of p94 Δ ex at N2A than at M, whereas full-length p94 is predominantly at M. This may indicate that p94 Δ ex have higher affinity to N2A than M at this stage. It is possible that the disappearance of p94 Δ ex from the N2A site enables p94 to gain access to it, which is important for myofibrils to mature fully.

In transgenic mice, overexpression of p94 Δ ex6 or p94 Δ ex15, but not full-length p94WT, blocked/delayed maturation of myofibers (34). These variants, which were shown to be less active than p94, especially with regard to autolytic activity (29), could act detrimentally at various developmental stages. Thus, these previous and our data are in support that both the transient expression and the disappearance of p94 isoforms at the early stages of myogenesis are important for

myotubes maturation, probably because these isoforms respond differently to the cellular mechanisms regulating p94. The differences in the threshold sarcomere lengths for the shift of localization from M to N2A—2.6 and 2.2 μm for p94^{WT} and p94 Δex6 ^{WT}, respectively—could be one indication of these effects.

Interaction between p94 and s- α -actinin

By YTH screening, the middle region of s- α -actinin, which encompasses the junction of two consecutive spectrin repeats and binds to the NS region of p94, was identified as the long-sought binding partner for p94 in Z. Direct interaction between s- α -actinin and NS, as well as full-length p94, was detected in COS7 cells. In yeast, however, the full-length s- α -actinin did not bind to p94, probably because full-length s- α -actinin tightly forms homodimers (35) and/or YTH sometimes shows false negative results. It should be noted that s- α -actinin showed a complicated fashion when binds to p94; i.e., s- α -actinin fragments (aa401-894; aa430-894) did not bind to p94 NS region, even though these fragments contain the region able to bind p94 (aa441-568). Similar to our results, it was reported that s- α -actinin showed intricate patterns when interacting with connectin (36). Therefore, although further study is required for determination of the precise p94 binding site in s- α -actinin, minimum p94 binding region so far determined is the C-terminal half of R2 plus the N-terminal half of R3 (Fig. 5K, red or pink region).

S- α -actinin is one of the major components of Z (37), and has multiple binding molecules,

such as α -actin (38), the N-terminal Z-repeat region of connectin (15,16), myopalladin (39), FATZ1/calsarcin-2/myozenin-1 (40), calsarcin-3/myozenin-3 (41), and cypher/ZASP/Oracle (42). Our finding of interaction between NS and s- α -actinin suggests that p94 also contributes to the integrity of Z. Consistently, previous studies showed that p94 antisense oligonucleotide treatment disrupted Z-band structures and diminished s- α -actinin detection (43). As the NS but not IS2 epitope was preferentially localized in Z during myofibrillogenesis, N-terminal proteolyzed fragment(s) of p94 could be important for this aspect.

p94 localization is affected by the sarcomere length and its proteolytic activity

The dynamic and distinct localization of exogenously expressed p94 relative to sarcomere length suggests that p94 senses myofibrillar stretch—when sarcomeres are becoming overextended, some portions of p94 may change localization from M to N2A (Fig. 9 C). In YTH, binding between p94 and connectin is much stronger in N2A than in M (29), and the N2A p94 binding site is close to extensible spring elements (PEVK) of connectin. Thus, extension of connectin may unmask N2A epitopes important for p94 binding, allowing p94 to be recruited from M to N2A and suggesting involvement of p94 in signal transduction pathways in myofibrils. This idea is supported by Trombitas's study, which showed that the change of sarcomere length up to ca. 2.5 μm is mainly by changes in IG structures, major motifs in N2A, and further stretch is by extension of PEVK (44).

Interestingly, active redistribution of T-cap/telethonin, one of the connectin ligands, from M to Z has also been suggested as a consequence of its phosphorylation by the connectin kinase domain (ttk) (45). As connectin filaments from opposite half-sarcomeres overlap in M, both the C-terminal is7 and ttk locate in the periphery of the M-line lattice (46). Thus, dissociation of p94 from M potentially can be linked by stretch-activated phosphorylation mediated by ttk. Our previously proposed “signal complex” hypothesizes that connectin-binding proteins in Z, N2A, or M function as a complex at each position to maintain cooperativity among the many different levels of muscle components, e.g., between the sarcomere and the nucleus (32), where the extension/contraction states in N2A would be communicated to other levels by the action of p94.

Localization of p94CS and p94 Δ ex:CS failed to reflect extension of sarcomere as promptly as their active counterparts do. This observation is significant in that it relates, for the first time, a defect in the proteolytic activity of p94 to its behavior within the physiological event of muscle extension/contraction. Our results indicate that protease-defective p94 cannot initiate or transfer the cellular response required for saving muscle from the enormous stresses posed during cycles of extension/contraction, which possibly leads to accumulated damage of muscle, resulting in a muscular dystrophy phenotype after some decades. Reported phenotypes in skeletal muscles of p94 null mice are consistent with the above

explanation; myofibrillogenesis occurs normally, but with misaligned thick filaments in the sarcomeres (6), and sarcomere remodeling, which is induced by unloading muscles, is impaired (47). Together with the late incorporation of p94 into myofibrils, these data suggest that p94 participates in the maintenance of sarcomere structures, which undergo deformation while the muscle is continuously used.

The most important question should be; what is p94 protease activity required for? One possibility is that it allows swift changes in p94 structure by autolysis. Autolysis of p94 has been shown to proceed by “nicking” in NS, IS1, and/or IS2 (21), with the reaction in IS2 regulated by N2A. These proteolytic modifications of p94 itself possibly result in a more “movable” conformation for p94, altering its affinity to connectin and other molecules. Consistent with this idea, exogenously expressed p94 and p94 Δ ex6, which show different autolytic profiles (29), were slightly different in their propensity to change localization between M to N2A. At present, one explanation for the sluggish but not absent response of p94CS—devoid of autolytic activity—to sarcomere length changes is that in our cultured myotubes, endogenous wild-type p94 can intramolecularly proteolyze p94CS. This is consistent with previous reports that p94 null mice showed more severe phenotypes than transgenic mice overexpressing p94CS did (5,7). To provide more insight into the physiological functions of p94, what property of p94 is involved in its response to sarcomere conditions and how it is achieved

should be elucidated.

REFERENCES

1. Goll, D. E., Thompson, V. F., Li, H., Wei, W., and Cong, J. (2003) *Physiol. Rev.* **83**, 731-801
2. Suzuki, K., Hata, S., Kawabata, Y., and Sorimachi, H. (2004) *Diabetes* **53**, S12-S18
3. Sorimachi, H., Imajoh-Ohmi, S., Emori, Y., Kawasaki, H., Ohno, S., Minami, Y., and Suzuki, K. (1989) *J. Biol. Chem.* **264**, 20106-20111
4. Richard, I., Broux, O., Allamand, V., Fougerousse, F., Chiannilkulchai, N., Bourg, N., Brenguier, L., Devaud, C., Pasturaud, P., Roudaut, C., Hillaire, D., Passos-Bueno, M.-R., Zats, M., Tischfield, J. A., Fardeau, M., Jackson, C. E., Cohen, D., and Beckmann, J. S. (1995) *Cell* **81**, 27-40
5. Tagawa, K., Taya, C., Hayashi, Y., Nakagawa, M., Ono, Y., Fukuda, R., Karasuyama, H., Toyama-Sorimachi, N., Katsui, Y., Hata, S., Ishiura, S., Nonaka, I., Seyama, Y., Arahata, K., Yonekawa, H., Sorimachi, H., and Suzuki, K. (2000) *Hum. Mol. Genet.* **9**, 1393-1402
6. Kramerova, I., Kudryashova, E., Tidball, J. G., and Spencer, M. J. (2004) *Hum. Mol. Genet.* **13**, 1373-1388
7. Richard, I., Roudaut, C., Marchand, S., Baghdiguan, S., Herasse, M., Stockholm, D., Ono, Y., Suel, L., Bourg, N., Sorimachi, H., Lefranc, G., Fardeau, M., Sebille, A., and Beckmann, J. S. (2000) *J. Cell Biol.* **151**, 1583-1590
8. Ono, Y., Shimada, H., Sorimachi, H., Richard, I., Saido, T. C., Beckmann, J. S., Ishiura, S., and Suzuki, K. (1998) *J. Biol. Chem.* **273**, 17073-17078
9. Tokuyasu, K. T., and Maher, P. A. (1987) *J. Cell Biol.* **105**, 2795-2801
10. Maruyama, K. (1976) *J. Biochem.* **80**, 405-407
11. Wang, K., McClure, J., and Tu, A. (1979) *Proc Natl Acad Sci U S A* **76**, 3698-3702
12. Labeit, S., and Kolmerer, B. (1995) *Science* **270**, 293-296
13. Obermann, W. M. J., Gautel, M., Steiner, F., Ven, P. F. M. v. d., Weber, K., and Furst, D. O. (1996) *J. Cell Biol.* **134**, 1441-1453
14. Ojima, K., Lin, Z. X., Zhang, Z. Q., Hijikata, T., Holtzer, S., Labeit, S., Sweeney, H. L., and Holtzer, H. (1999) *J. Cell Sci.* **112**, 4101-4112
15. Ohtsuka, H., Yajima, H., Maruyama, K., and Kimura, S. (1997) *FEBS Lett.* **401**, 65-67
16. Sorimachi, H., Freiburg, A., Kolmerer, B., Ishiura, S., Stier, G., Gregorio, C. C., Labeit, D., Linke, W. A., Suzuki, K., and Labeit, S. (1997) *J. Mol. Biol.* **270**, 688-695
17. Gregorio, C. C., Trombitas, K., Centner, T., Kolmerer, B., Stier, G., Kunke, K.,

- Suzuki, K., Obermayr, F., Herrmann, B., Granzier, H., Sorimachi, H., and Labeit, S. (1998) *J. Cell Biol.* **143**, 1013-1027
18. Centner, T., Yano, J., Kimura, E., McElhinny, A. S., Pelin, K., Witt, C. C., Bang, M. L., Trombitas, K., Granzier, H., Gregorio, C. C., Sorimachi, H., and Labeit, S. (2001) *J. Mol. Biol.* **306**, 717-726
 19. Sorimachi, H., Kinbara, K., Kimura, S., Takahashi, M., Ishiura, S., Sasagawa, N., Sorimachi, N., Shimada, H., Tagawa, K., Maruyama, K., and Suzuki, K. (1995) *J. Biol. Chem.* **270**, 31158-31162
 20. Haravuori, H., Vihola, A., Straub, V., Auranen, M., Richard, I., Marchand, S., Voit, T., Labeit, S., Somer, H., Peltonen, L., Beckmann, J. S., and Udd, B. (2001) *Neurology* **56**, 869-877
 21. Ono, Y., Torii, F., Ojima, K., Doi, N., Yoshioka, K., Kawabata, Y., Labeit, D., Labeit, S., Suzuki, K., Abe, K., Maeda, T., and Sorimachi, H. (2006) *J. Biol. Chem.* **281**, 18519-18531
 22. Taveau, M., Bourg, N., Sillon, G., Roudaut, C., Bartoli, M., and Richard, I. (2003) *Mol. Cell. Biol.* **23**, 9127-9135
 23. Ojima, K., Uezumi, A., Miyoshi, H., Masuda, S., Morita, Y., Fukase, A., Hattori, A., Nakauchi, H., Miyagoe-Suzuki, Y., and Takeda, S. (2004) *Biochem. Biophys. Res. Commun.* **321**, 1050-1061
 24. Sorimachi, H., Toyama-Sorimachi, N., Saido, T. C., Kawasaki, H., Sugita, H., Miyasaka, M., Arahata, K., Ishiura, S., and Suzuki, K. (1993) *J. Biol. Chem.* **268**, 10593-10605
 25. Trombitas, K., Greaser, M., Labeit, S., Jin, J. P., Kellermayer, M., Helmes, M., and Granzier, H. (1998) *J. Cell Biol.* **140**, 853-859
 26. Hackman, P., Vihola, A., Haravuori, H., Marchand, S., Sarparanta, J., De Seze, J., Labeit, S., Witt, C., Peltonen, L., Richard, I., and Udd, B. (2002) *Am J Hum Genet* **71**, 492-500
 27. Sadler, J. E. (1998) *Annu. Rev. Biochem.* **67**, 395-424
 28. Sato, N., Kawahara, H., Toh-e, A., and Maeda, T. (2003) *Mol. Cell. Biol.* **23**, 6662-6671
 29. Herasse, M., Ono, Y., Fougerousse, F., Kimura, E., Stockholm, D., Beley, C., Montarras, D., Pinset, C., Sorimachi, H., Suzuki, K., Beckmann, J. S., and Richard, I. (1999) *Mol. Cell. Biol.* **19**, 4047-4055
 30. Farkas, A., Tompa, P., and Friedrich, P. (2003) *Biol. Chem.* **384**, 945-949
 31. Kinbara, K., Sorimachi, H., Ishiura, S., and Suzuki, K. (1997) *Arch. Biochem. Biophys.* **342**, 99-107
 32. Witt, C. C., Ono, Y., Puschmann, E., McNabb, M., Wu, Y., Gotthardt, M., Witt, S. H., Haak, M., Labeit, D., Gregorio, C. C., Sorimachi, H., Granzier, H., and Labeit, S.

- (2004) *J. Mol. Biol.* **336**, 145-154
33. Holtzer, H., Hijikata, T., Lin, Z. X., Zhang, Z. Q., Holtzer, S., Protasi, F., Franzini-Armstrong, C., and Sweeney, H. L. (1997) *Cell Struct. Funct.* **22**, 83-93
 34. Spencer, M. J., Guyon, J. R., Sorimachi, H., Potts, A., Richard, I., Herasse, M., Chamberlain, J., Dalkilic, I., Kunkel, L. M., and Beckmann, J. S. (2002) *Proc. Natl. Acad. Sci. USA* **99**, 8874-8879
 35. Djinovic-Carugo, K., Young, P., Gautel, M., and Saraste, M. (1999) *Cell* **98**, 537-546
 36. Young, P., Ferguson, C., Banuelos, S., and Gautel, M. (1998) *EMBO J.* **17**, 1614-1624
 37. Endo, T., and Masaki, T. (1984) *J. Cell Biol.* **99**, 2322-2332
 38. Goll, D. E., Dayton, W. R., Singh, I., and Robson, R. M. (1991) *J. Biol. Chem.* **266**, 8501-8510
 39. Bang, M. L., Mudry, R. E., McElhinny, A. S., Trombitas, K., Geach, A. J., Yamasaki, R., Sorimachi, H., Granzier, H., Gregorio, C. C., and Labeit, S. (2001) *J. Cell Biol.* **153**, 413-427
 40. Takada, F., Vander Woude, D. L., Tong, H. Q., Thompson, T. G., Watkins, S. C., Kunkel, L. M., and Beggs, A. H. (2001) *Proc. Natl. Acad. Sci. USA* **98**, 1595-1600
 41. Frey, N., and Olson, E. N. (2002) *J. Biol. Chem.* **277**, 13998-14004
 42. Zhou, Q., Ruiz-Lozano, P., Martone, M. E., and Chen, J. (1999) *J. Biol. Chem.* **274**, 19807-19813
 43. Poussard, S., Duvert, M., Balcerzak, D., Ramassamy, S., Brustis, J. J., Cottin, P., and Ducastaing, A. (1996) *Cell Growth Differ.* **7**, 1461-1469
 44. Trombitas, K., Wu, Y., McNabb, M., Greaser, M., Kellermayer, M. S., Labeit, S., and Granzier, H. (2003) *Biophys. J.* **85**, 3142-3153
 45. Mayans, O., van der Ven, P. F., Wilm, M., Mues, A., Young, P., Furst, D. O., Wilmanns, M., and Gautel, M. (1998) *Nature* **395**, 863-869
 46. Obermann, W. M. J., Gautel, M., Weber, K., and Furst, D. O. (1997) *EMBO J.* **16**, 211-220
 47. Kramerova, I., Kudryashova, E., Venkatraman, G., and Spencer, M. J. (2005) *Hum. Mol. Genet.* **14**, 2125-2134
 48. Kawabata, Y., Hata, S., Ono, Y., Ito, Y., Suzuki, K., Abe, K., and Sorimachi, H. (2003) *FEBS Lett.* **555**, 623-630

FOOTNOTES

We are grateful to Tatsuya Maeda, Muriel Herasse, and Isabelle Richard for generous gifts of cDNA constructs, and to Takuro Arimura, Akinori Kimura, and all of the Calpain PT members for experimental support and valuable discussion. This work was supported in part by

MEXT.KAKENHI 16026209, 17028055, and 18076007 (to HS), JSPS.KAKENHI 18700392 (to KO), 18770124 (to YO), and 18380085 (to HS), Research Grant (17A-10) for Nervous and Mental Disorders from the Ministry of Health, Labor and Welfare (to HS), Sasagawa Scientific Research Grant from The Japan Science Society (to KO) and the DFG (La668/7-2) (to SL).

The abbreviations used are: IS1 and IS2, specific insertion sequences 1 and 2 of p94; MHC, myosin heavy chain; NS, N-terminal specific sequence of p94; p94CS, p94:C129S protease-inactive mutant; PEVK, Pro, Glu, Val, and Lys-rich spring elements of connectin; PM, proliferating presumptive myoblast; s- α -actinin, sarcomeric α -actinin (α -actinin 2); ttk, titin/connectin kinase domain; YTH, yeast two-hybrid.

FIGURE LEGENDS

Figure 1. Analysis of the expression of p94 and its splicing variants during myogenesis. (A) A schematic domain structure of p94, the antigens for the antibodies, and the exon structures amplified by RT-PCR. NS, IS1, and IS2 are p94-specific insertion sequences. Domains IIa+IIb, III, and IV, are the conserved calpain domains. Most of IS1 and IS2 are encoded by exon 6 and exons 15 and 16, respectively. The expected sizes of the RT-PCR products are shown. (B) The expression of embryonic MHC and desmin were analyzed by Western blotting. As skeletal muscle differentiation proceeds, the expression of embryonic MHC relative to desmin decreases. (C–F) RT-PCR analysis of p94 transcripts using primer sets for amplification of exons 1 to 24 (C), 4 to 9 (D), 10 to 17 (E), and 4 to 17 (F). Arrows and open arrowheads correspond to the transcripts with no exons skipped and those with exon skipping, respectively (C to F). Note that the skipping of exon 6 or exons 15 and 16 were not discernible from each other in transcripts covering exons 4 to 17 (F, upper open arrowhead). (G) Stable expression of the μ -calpain large subunit during myogenesis. (H) Detection of p94 protein in cell lysates using a p94-specific anti-pIS2C antibody. Full-length p94 and its proteolytic fragments are indicated by the arrow and closed arrowheads, respectively. The open arrowheads indicate p94 fragments, which could be p94 Δ ex6, 15 and/or 16. (I) Expression of p94 Δ ex15/16 protein during differentiation detected with an affinity-purified anti-p Δ ex15/16 antibody. The open and closed arrowheads indicate p94 Δ ex15/16 and its possible proteolytic fragments, respectively. Lanes in panels (B)–(I): H₂O, negative control; PM, proliferating presumptive myoblasts; Day 1, 3, 6, 10, and 13, cells differentiated for the indicated number of days; QC, Sol, and TA, quadriceps femoris, soleus, and tibialis anterior muscles, respectively from a 15-week-old C57BL6 mouse; p94:CS and p94:ex15⁻16⁻, proteins recombinantly expressed in COS7 cell.

Figure 2. Expression of transcripts corresponding to the p94 binding sites of connectin in the N2A and M-line regions. (A) A single connectin molecule spans from the Z-band to the M-line.

The locations of the amplified regions in connectin by RT-PCR are schematically represented in sarcomere structure (bars). The double-headed arrows correspond to the p94 binding sites. The antigens for the anti-connectin N2A and M8M9 antibodies are indicated by brackets. I and M, together with the numbers, indicate the immunoglobulin motifs in the I-band and the M-line, respectively; PEVK, kinase, and is7 indicate the PEVK region, the kinase domain, and the insertion sequences, respectively. Expression of transcripts corresponding to the p94 binding sites in the N2A region (B) and the M-line (C) was analyzed by RT-PCR. The arrows and the open arrowhead indicate products corresponding to the transcripts with and without the p94 binding region as shown in (A).

Figure 3. Colocalization of p94 with connectin at the N2A region or the M-line in the late but not in the early stage of myofibrillogenesis. Cultured skeletal muscle cells at day 3 (A–I) and day 10 (J–R) were stained with the anti-pIS2C antibody (B, E, H, K, N, and Q) in combination with one of the antibodies against α -actinin (A and J), connectin N2A (D and M), or connectin M8M9 (G and P). Nuclei were stained with TOTO3 (blue; A–I). Merged images are shown at the right (C, F, I, L, O, and R). Brackets indicate the areas of the growth tips. At day 3, α -actinin showed stress-fiber-like structures in a growth tip and the Z-band striation (arrows) in the shaft of myotubes (A and C). N2A (D and F), and M-line (G and I) striations were observed in the shaft of myotubes (arrows). p94 was detected in a granular structure in the cytosol and was not colocalized with α -actinin, and connectin N2A and M-line regions (A–I). p94 signals were also detected in myonuclei (B, C, H, and I). At day 10 myotubes, arrowheads and brackets indicate p94 localization, whereas arrows indicate the localization of α -actinin (J and L), connectin N2A (M and O), and connectin M8M9 (P and R). Insets show magnified images (J–R). Bars, 10 μ m.

Figure 4. Localization of the p94 isoform p94 Δ ex15/16 in the sarcomere.

In cultured myotubes at day 6, localization of p94 Δ ex15/16 was examined using an anti-p Δ ex15/16 antibody (B, E, and H) in combination with an anti- α -actinin antibody (A, D, and G). Merged images are shown at the right (C, F, and I). D–I are these images at higher magnification. Localization of p94 Δ ex15/16 was observed as thick stripes at the Z-bands (E and F, brackets), as dotted lines between the Z-bands (E and F, arrowheads), and doublets around the Z-bands (H and I, closed arrowheads). p94 Δ ex15/16 also accumulated as small particles in the cytosol of the shafts of juvenile myotubes (asterisk). Arrows indicate the Z-band localization of α -actinin. In the merged image, nuclei (blue) were stained with DAPI (C). Bars, 10 μ m.

Figure 5. Z-band localization of p94 and its interaction with α -actinin at the NS domain.

(A–C) Localization of p94 was examined in cultured myotubes at day 6 using an anti-pNS antibody. p94 colocalized with α -actinin at Z (arrowhead, B and C). (D–I) In longitudinal cryostat sections of EDL muscles from six-month-old C57BL/6 mice, p94 was detected with anti-pIS2C (E) or

anti-pNS (H) antibodies, and Z was detected with an anti-s- α -actinin antibody (D and G, arrows). In adult muscles, in contrast to day 6 myotubes, p94 was observed in both N2A and M (E, F, H, and I, closed and open arrowheads, respectively) with both anti-pIS2C and anti-pNS antibodies. p94 was also detected in Z using an anti-NS antibody (H and I, *), but was less clear with anti-pIS2C (E, *). Bars, 10 μ m. (J) A schematic for the domain structure of s- α -actinin and its interaction with p94 NS as detected by YTH assay. S- α -actinin consists of an N-terminal actin-binding domain, four spectrin-like repeat domains, and tandem EF-hand motifs in the C-terminal region. The p94 NS binding site in s- α -actinin was located between the centers of the second and third spectrin-like repeat domains (aa: 441–568; double-headed arrow). (K) Ribbon presentation of the s- α -actinin spectrin-repeat region. The two antiparallel subunits of the s- α -actinin spectrin-repeat region are depicted in blue and green. Minimum p94 binding region (aa441-568) is shown in red or pink. Ribbon diagrams were generated using MolFeat Ver.2.2 3D imaging software (FiatLux Inc., Tokyo, Japan).

Figure 6. Interaction between p94 and s- α -actinin in mammalian culture cells. (A and B) Myc-tagged s- α -actinin and Flag-tagged p94CS coexpressed in COS7 cells were examined for their interaction. Myc-tagged s- α -actinin was coimmunoprecipitated with Flag-tagged p94CS (A, arrowhead). Alternatively, Flag-tagged p94CS was detected in the sample immunoprecipitated with the anti-Myc antibody (B, arrowhead). Coimmunoprecipitation of GFP-tagged p94 NS domain and Myc-tagged s- α -actinin was also detected (C and D, arrowheads). Therefore, the interaction between p94 and full-length s- α -actinin was shown to occur via the p94 NS region in mammalian cells. IP, immunoprecipitation; WB, western blot.

Figure 7. Dynamic translocation of exogenously expressed p94 in relation to sarcomere condition. At day 6 after transfection, myotubes expressing either Flag-tagged p94WT (A–C, G–I), Flag-tagged p94CS (D–F), or Flag-p94 Δ ex6:CS (J–O), were doubly immunostained with anti-Flag (B, E, H, K, and N) and anti-M8M9 antibodies (A, D, G, J, and M). Merged images are shown at the right (C, F, I, L and O), with nuclei stained with DAPI shown in blue. Transfected myotubes (G–O) showed hyperextension (right side in G–I, and left side in J–O) and hypercontraction (left side in G–I, and right side in J–L). (M–O) High magnification views of the border areas (J–L, rectangle) are shown. Closed arrows indicate M. Closed and open arrowheads indicate signals for exogenously expressed Flag-p94 at M and N2A, respectively. *, untransfected myotubes. Bars, 10 μ m.

Figure 8. Quantitative analysis of the M-line and N2A localization of exogenously expressed p94. At day 6 after transfection, the localization of Flag-p94WT, Flag-p94CS, Flag-p94 Δ ex6:WT and Flag-p94 Δ ex6:CS was evaluated (see Materials and methods). The sarcomere length between the centers of connectin M8M9 positive signals corresponding to the M-lines was measured using Zeiss LSM imaging software. Black and gray bars indicate the ratios of Flag-p94 localization in the

M-lines and the N2A regions, respectively.

Figure 9. Expression and localization of p94 in the context of myofibril development and sarcomere function. (A) Developmental changes in the expression and localization of p94 and its isoforms are summarized. I) At the early stage of myofibrillogenesis, the N- and C-termini of connectin are associated with I-Z-I bodies and thick filaments, respectively. At this stage, p94 and its isoforms are distributed in the cytosol (Cyt) as small punctuate structures. II) The sarcomere scaffold is assembled, that is, interdigitating Z, N2A and M structures are formed. Most of the p94 remains in the cytosol, with some populations of p94 and isoforms targeted to Z and/or N2A/M. III) Later, p94 is incorporated into Z, N2A, and M. p94 isoforms tend to be targeted to N2A rather than to M. IV) In adult skeletal muscles, p94 isoforms were absent, and p94 localizes in Z/N2A/M. The structures of p94 and its isoforms are schematically shown; the gray domain might be proteolytically removed. Localization and relative ratios of p94 and its isoforms at specific regions, and the signals with each antibody are qualitatively summarized. (B) Qualitative profiles of p94 Δ ex/p94 ratios in the four positions during myofibrillogenesis as discussed in (A) is shown. (C) A proposed model of p94 translocation in response to over and under stretching of muscle. In the range of normal contraction–stretching conditions, exogenously expressed p94 is located in the M-lines. When sarcomeres are over stretched, p94 accumulates in the N2A regions, being released from the M-lines and/or recruited from cytosol.

Table I. Primers for RT-PCR detection of p94, splicing variants of p94, connectin/titin, and μ -calpain

Primer	sense (5'–3')	antisense (5'–3')
p94 Exon 1 –Exon 24	atcgagctcggatcc-ATGCCAACTGTTATT AGT*	GGTTCAGGCATACATGGT
p94 Exon 4 –Exon 9	AACCACCGCAATGAGTTCTGG	TGTCCACAAAGCTCCAGTCC
p94 Exon 4 –Exon 17	AACCACCGCAATGAGTTCTGG	tccccgggtca-TTGTTGCTGTTCCCTCA CTTTCC*
p94 Exon 10 –Exon 17	ATAAGCTTCAGACCTGGACG	tccccgggtca-TTGTTGCTGTTCCCTCA CTTTCC*
connectin/ titin N2A	AAGGTACCAACCACTGCCACGTTT ATTGCAA	AAAGGATCTTTTTTTCACACCCTTT TTGGTCA
connectin/ titin M9M10	CGTGTACACTCTTGAAATCC	CTTCCTTGTTGTTCTTGGTTTTGG
μ -calpain	GAATTGGAATACCACATTTTACGA GG	TCAAAGGTCACAACACCATCCAG G

*These primers are as same as used in (48). The additional unrelated sequences were for cloning purposes.

Figure 1 (Ojima, K. et al.)

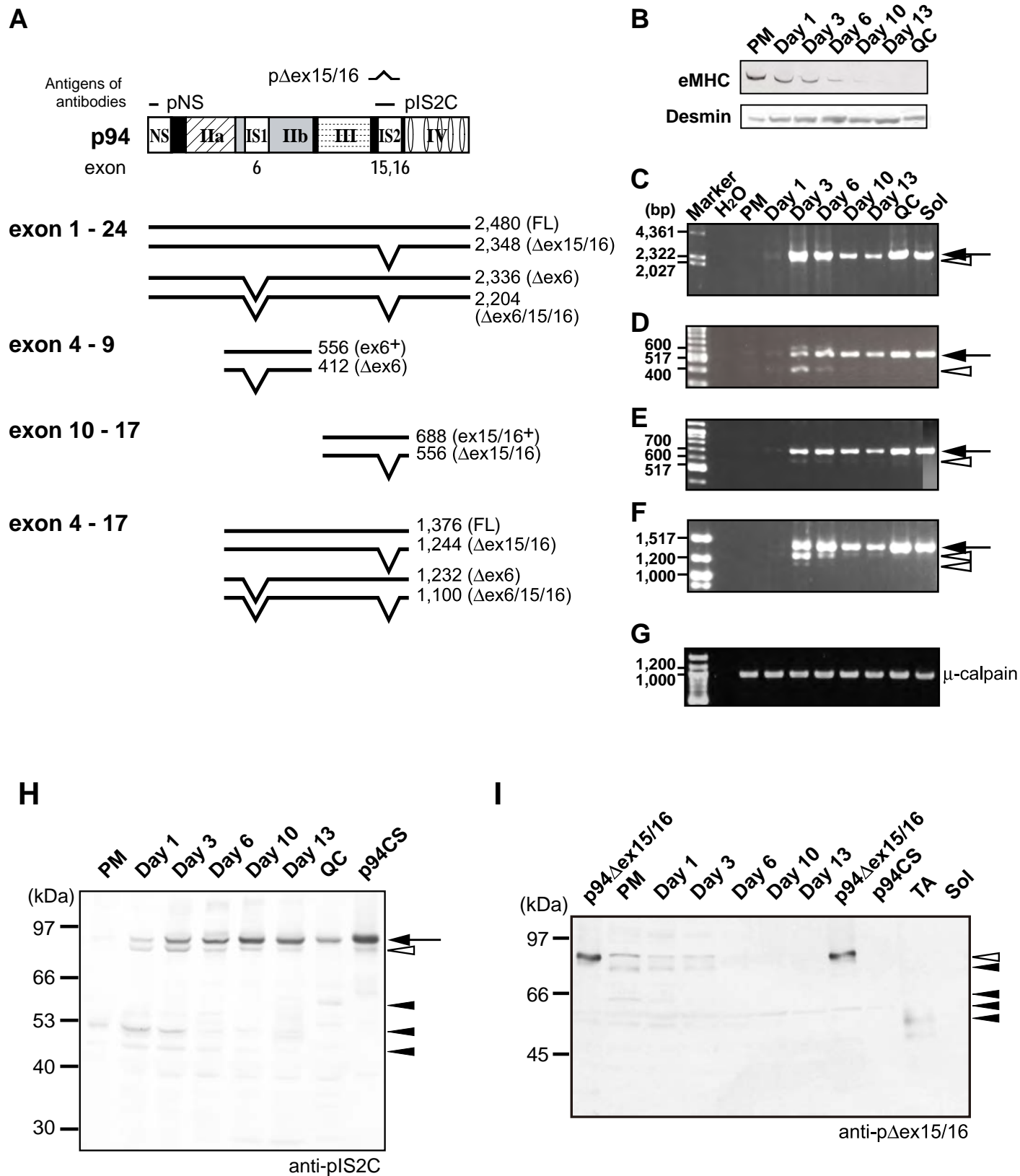


Figure 2 (Ojima, K. *et al.*)

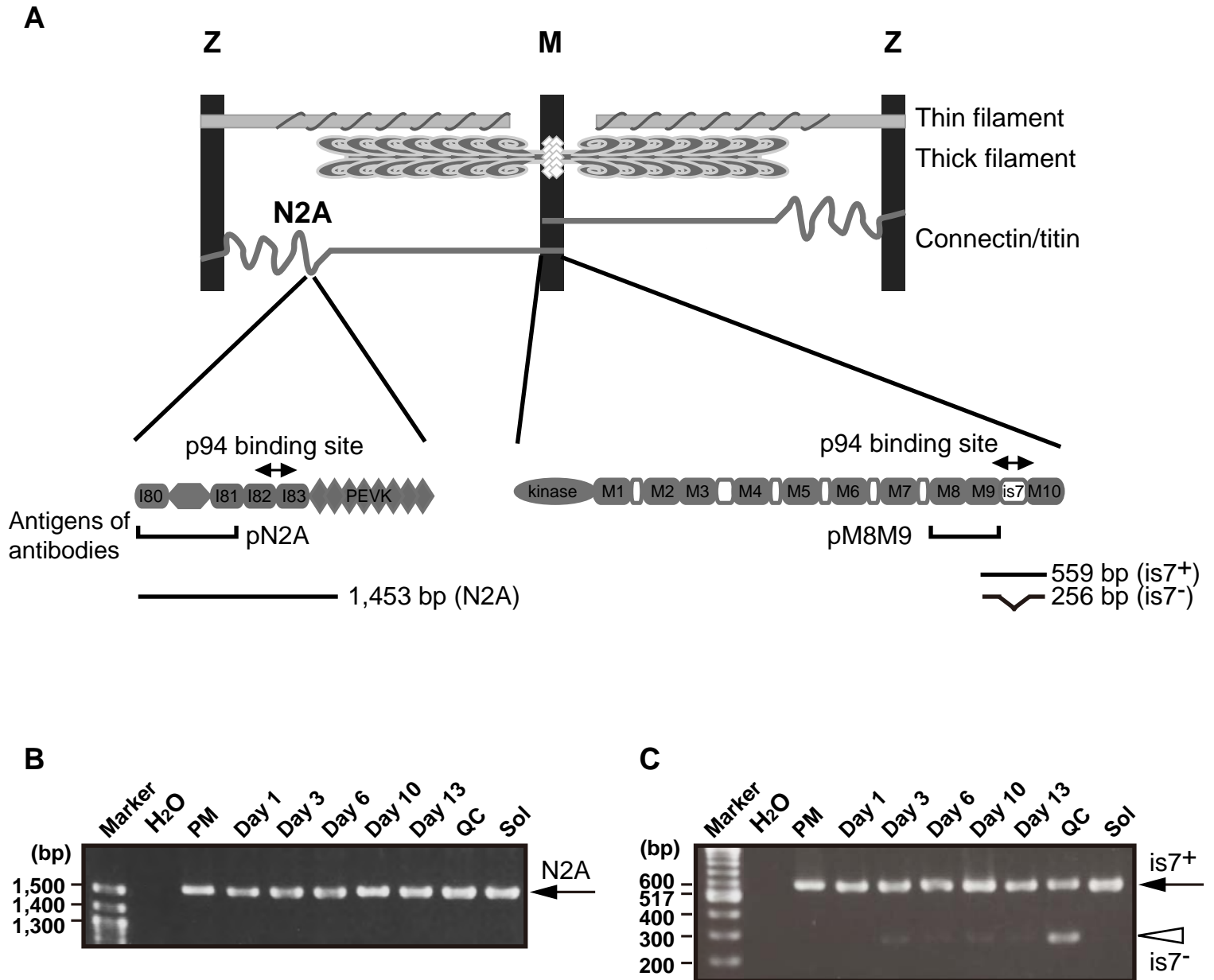


Figure 3 (Ojima, K. et al.)

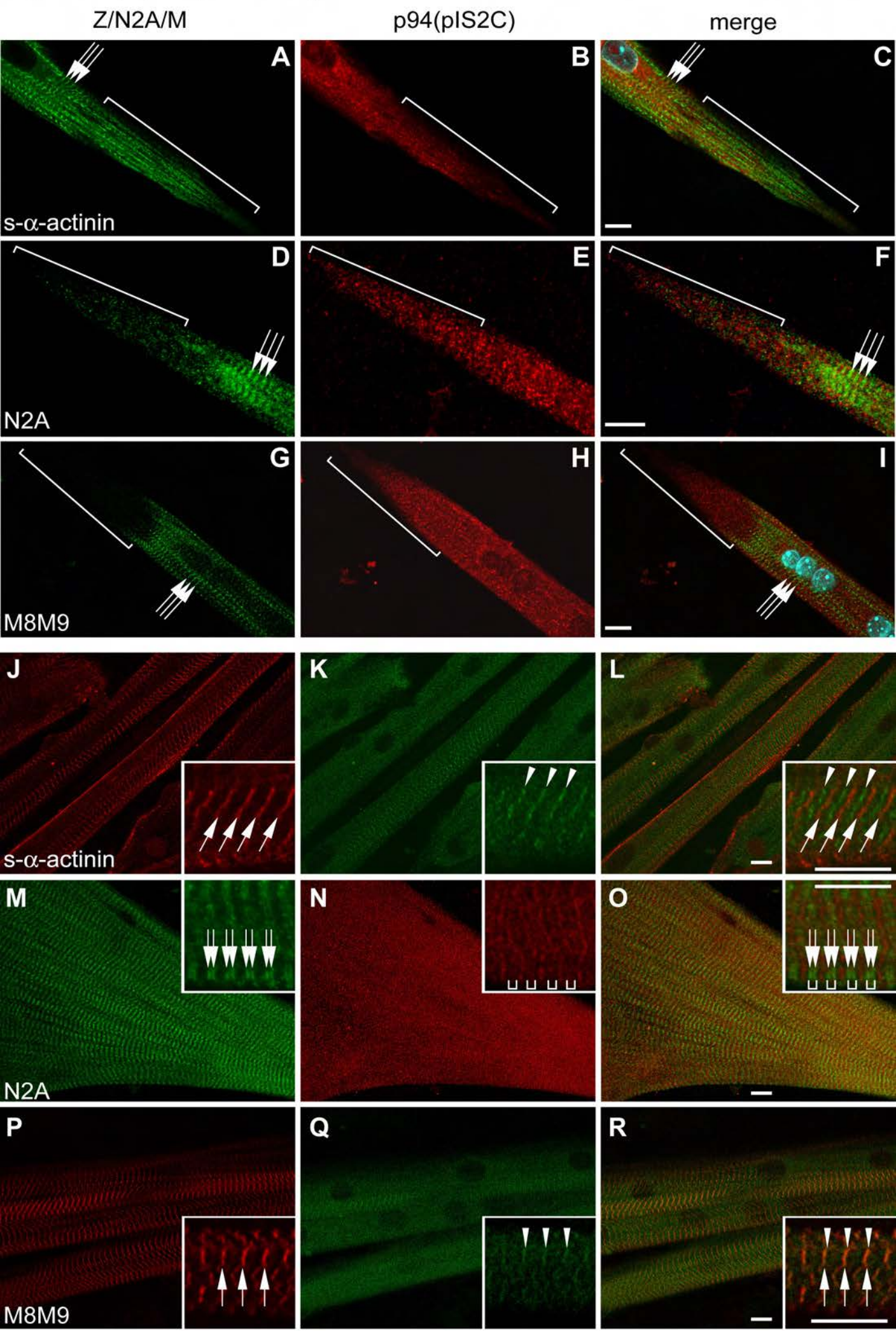


Figure 4 (Ojima, K. *et al.*)

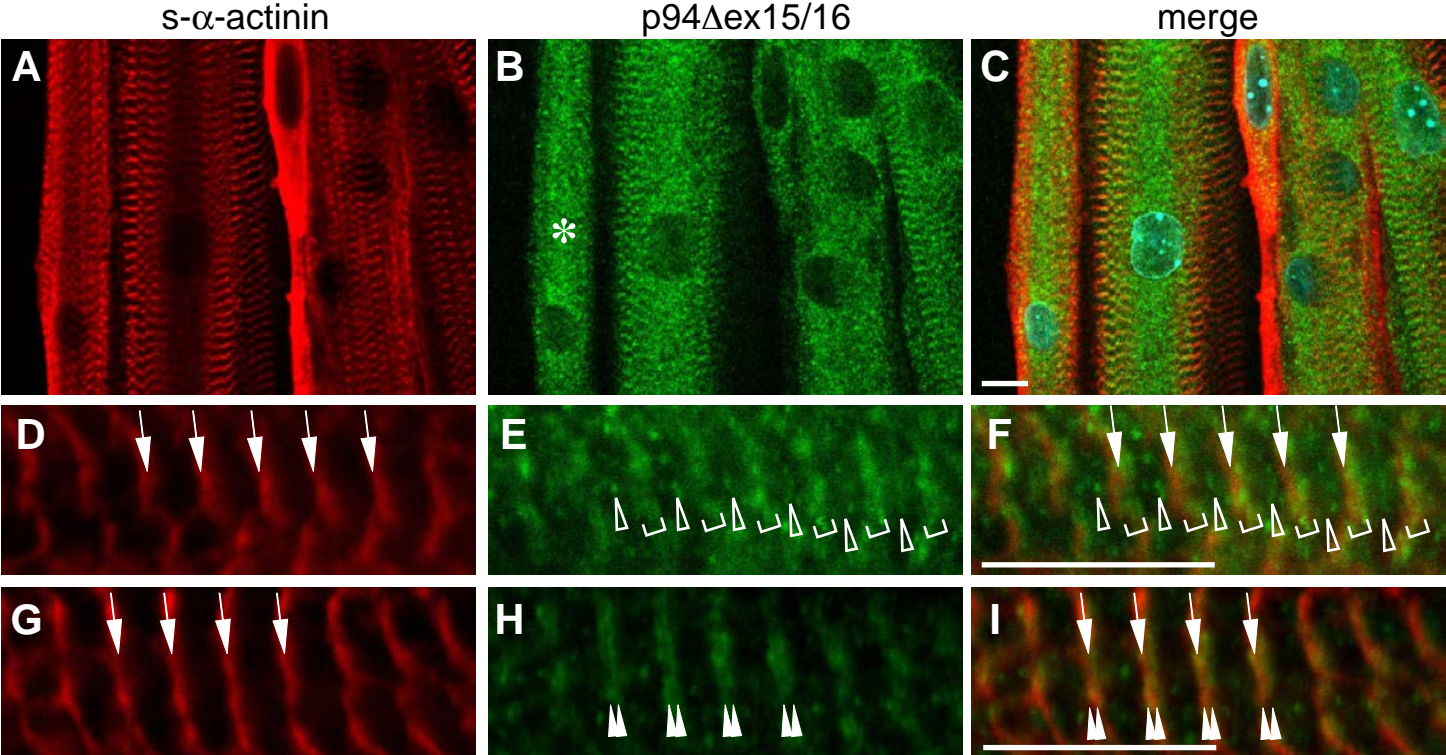


Figure 5 (Ojima, K. *et al.*)

s- α -actinin

p94

merge

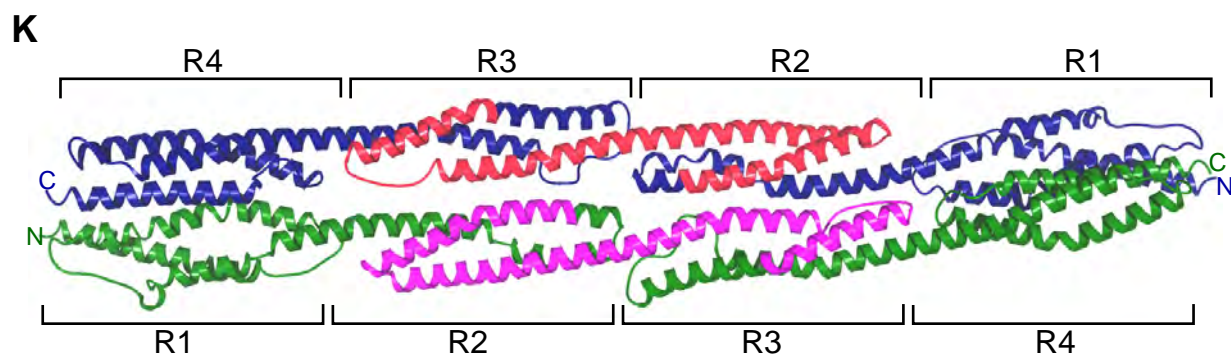
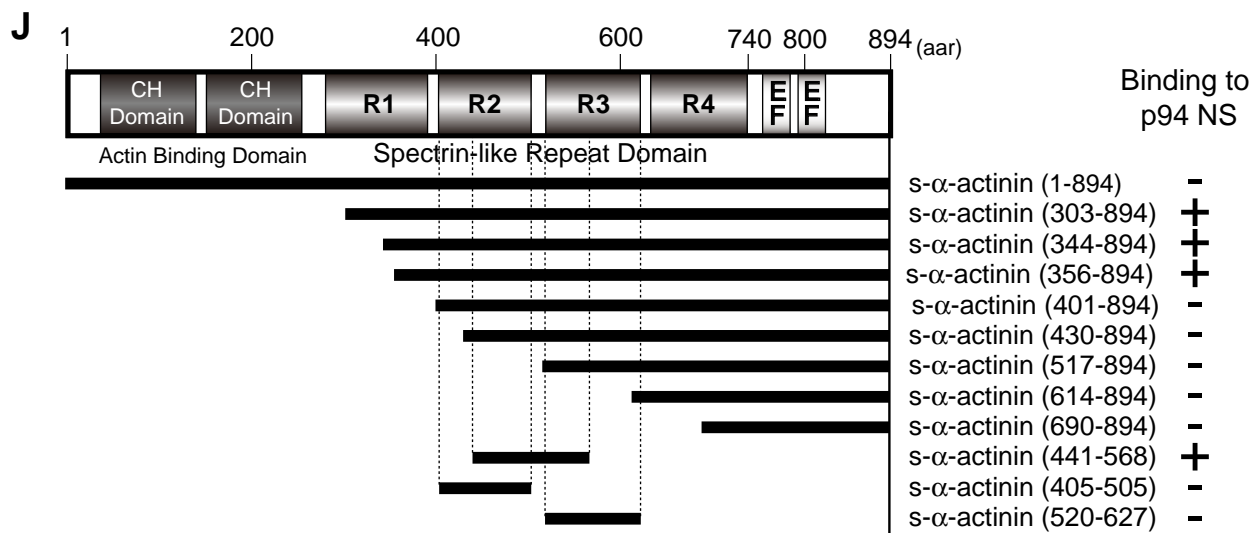
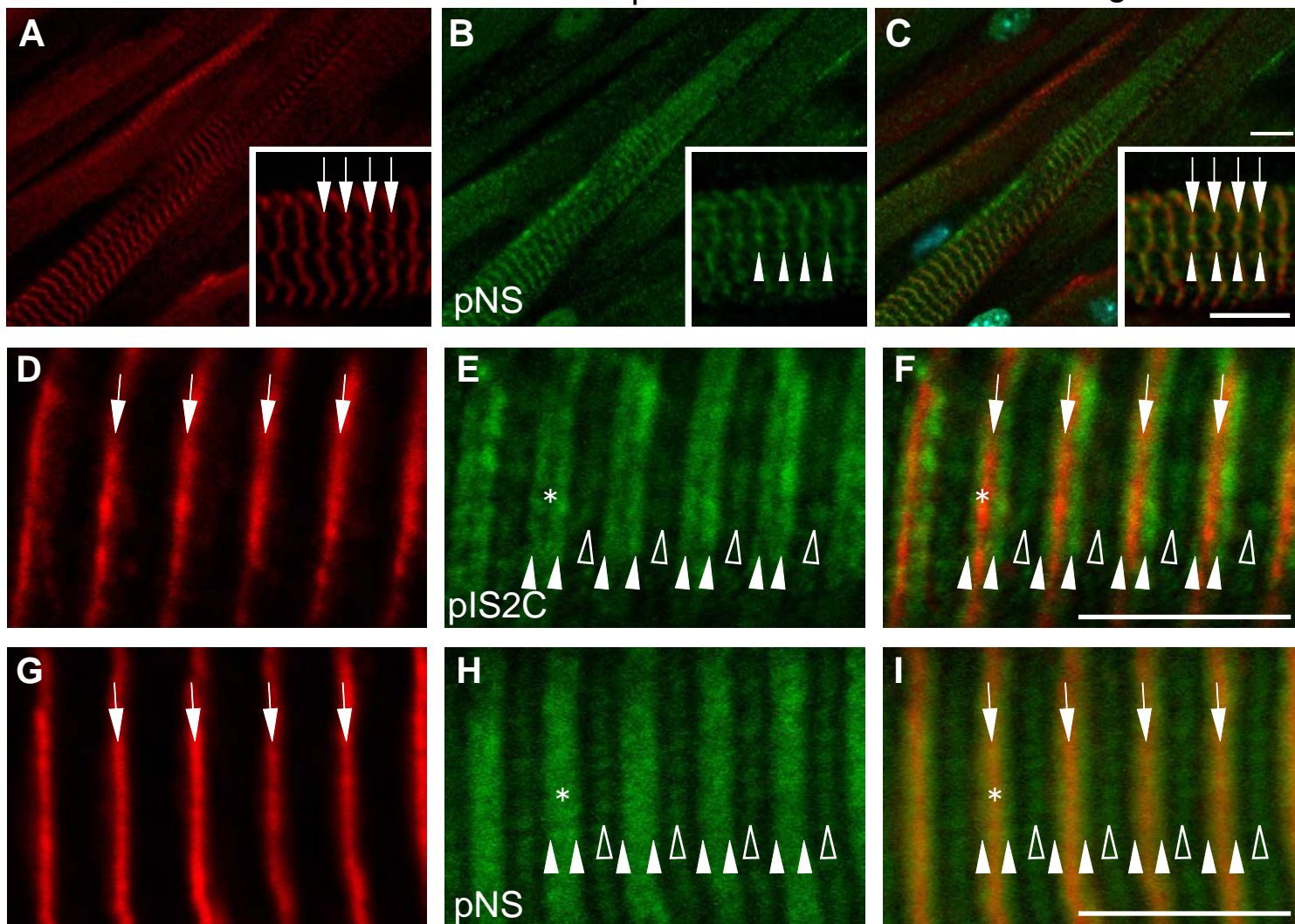
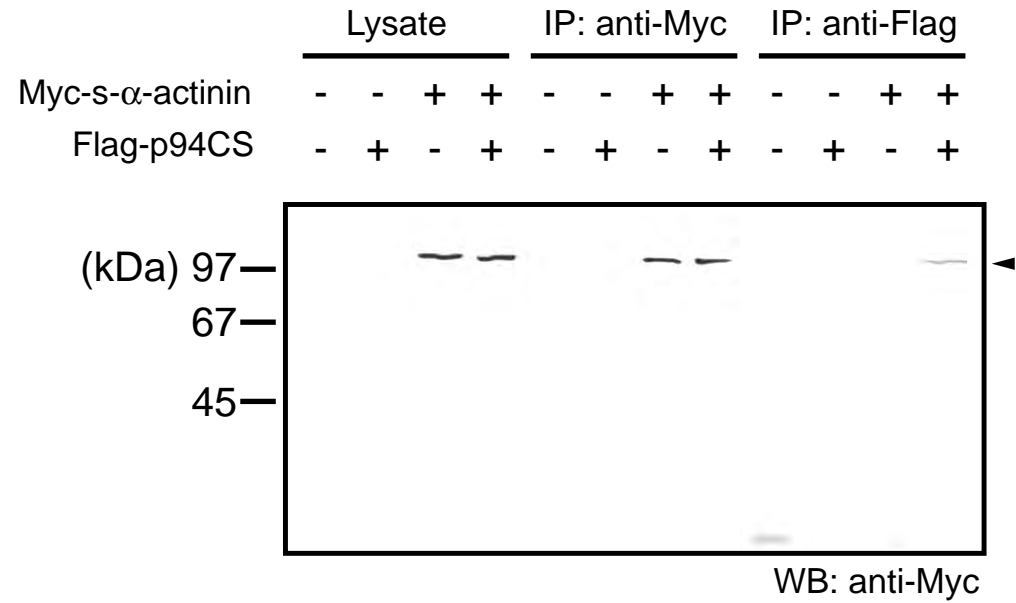
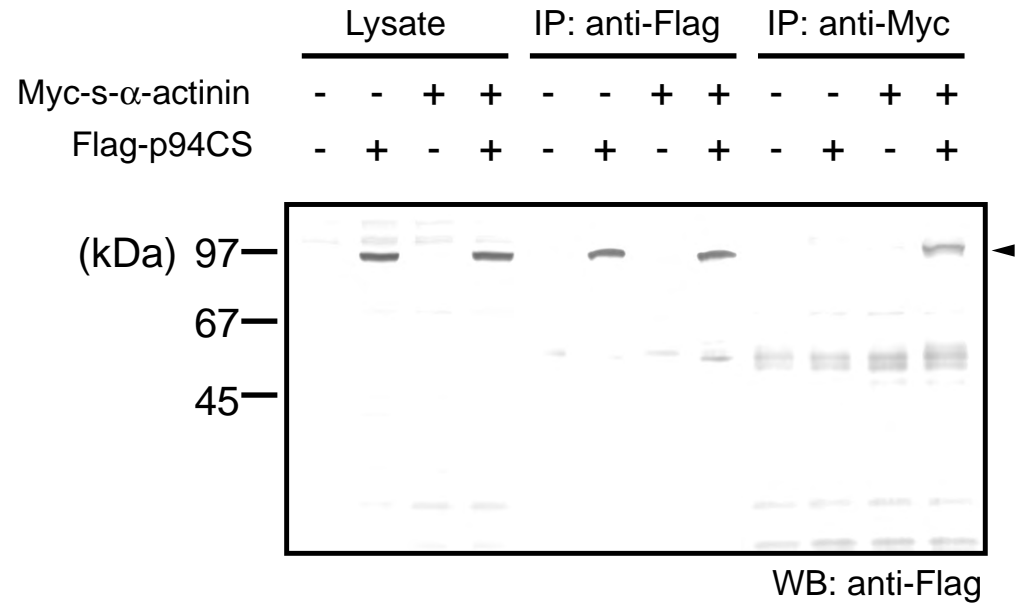


Figure 6 (Ojima, K. *et al.*)

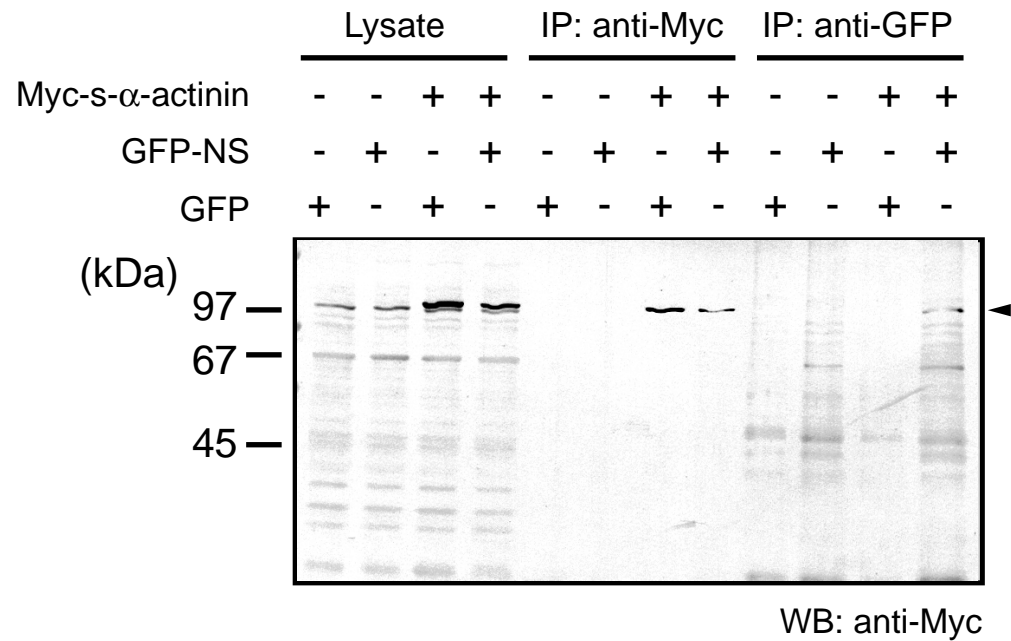
A



B



C



D

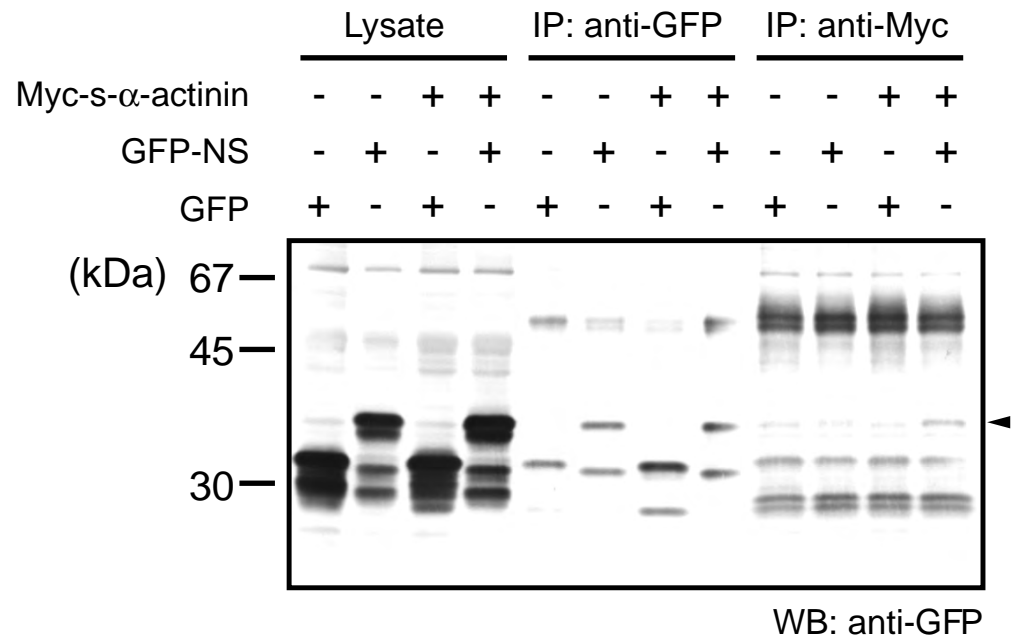


Figure 7 (Ojima, K. *et al.*)

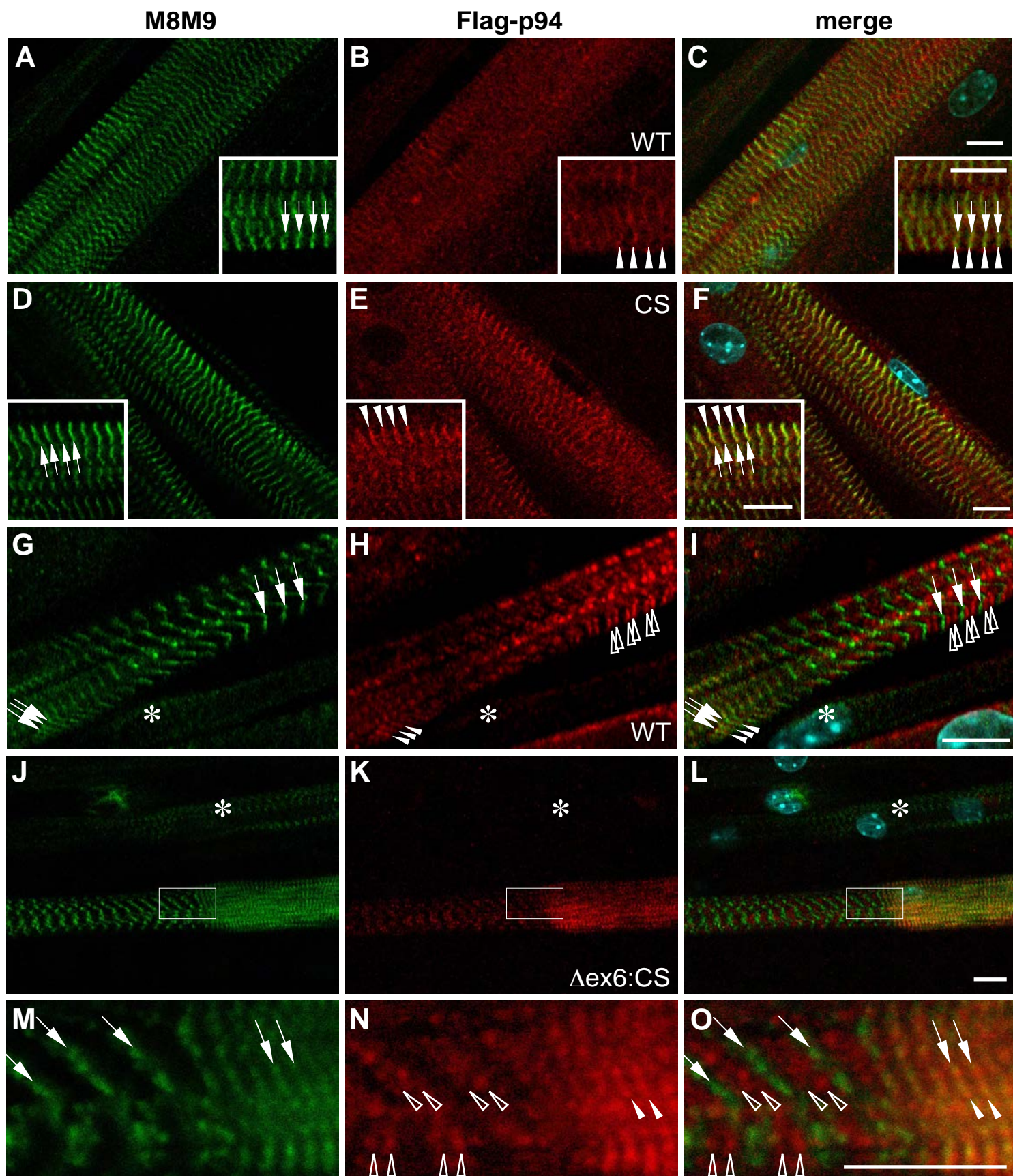


Figure 8 (Ojima, K. *et al.*)

